

# Medium effects of charged-hadron production in $p + Pb$ and $Pb + Pb$ collisions at LHC energies using modified Tsallis distribution

Kapil Saraswat<sup>1</sup>, Prashanta Kumar Khandai<sup>2</sup>, Deependra Singh Rawat<sup>3</sup>,  
and Venktesh Singh<sup>4</sup>

<sup>1</sup>*Institute of Physics, Academia Sinica, Taipei 11529, Taiwan*

*\*E-mail: drkapilsaraswat@zohomail.com*

<sup>2</sup>*Department of Physics, Ewing Christian College, Prayagraj 211003, India*

*\*E-mail: pkkhandai@gmail.com*

<sup>3</sup>*School of Allied Sciences (Physics), Graphic Era Hill University, Bhimtal Campus, Sattal Road, Nainital 263132 India*

*\*E-mail: dsrawatphysics@gmail.com*

<sup>4</sup>*Department of Physics, School of Physical & Chemical Science, Central University of South Bihar, Gaya 428236, India*

*\*E-mail: venktesh@cusb.ac.in*

.....  
The transverse momentum ( $p_T$ ) spectra of charged hadrons in  $p + p$ ,  $p + Pb$  and  $Pb + Pb$  collisions at  $\sqrt{s_{NN}} = 5.02$  TeV are presented here within the rapidity range of  $-2.5 < y < 2.0$ . We study the medium effects, which is produced by heavy ion collisions, on the behaviour of charged hadrons, by using a phenomenological fit function. These effects are attributed to two main factors: the transverse collective flow and the the energy loss of charged hadrons due to multiple scatterings. We observe the transverse collective flow at low and intermediate  $p_T$  region and the energy loss at high  $p_T$  region. Here we take all the published data from the ATLAS collaboration.  
.....

Subject Index      Charged hadron spectra, Quark Gluon Plasma, Collective Flow, Energy loss

# 1 Introduction

The RHIC (Relativistic Heavy Ion Collider) [1, 2] and the LHC (Large Hadron Collider) [3] are designed to study an elusive state of matter known as Quark Gluon Plasma (QGP) [4]. The QGP is a thermalized state of matter where quarks and gluons are deconfined and free to move independently. Scientists believe that such a state would have existed in the early Universe shortly after the Big Bang [5, 6]. There are many heavy-ion collisions performed at RHIC such as  $Au + Au$ ,  $Cu + Cu$ ,  $Cu + Au$  etc and many at LHC as  $Pb + Pb$ ,  $Xe + Xe$  etc. The  $p + p$  collisions are taken as a baseline for collisions involving heavy ions [7]. The particles produced in both  $p + p$  and heavy ion ( $A + A$ ) collisions are the results of multiple scatterings among partons. The distribution of  $p_T$  spectra in  $p + p$  collisions provides insights into the state of the matter when particles stop interacting at freeze-out state. Recent high-multiplicity  $p + p$  collisions data from the LHC [8, 9] predicts the formation of a quark-gluon plasma-like medium.

In high energy collisions between heavy ions (like lead or gold), the momentum distribution of emitted hadrons exhibits extra effects that happen after the initial collision. These effects include the collective flow [10] of hadrons, caused by the expansion of a hot [11, 12], dense matter formed in the collision and jet quenching [13], where high energy sprays of particles lose energy as they travel through the dense environment.

In  $p + p$  collisions, researchers analyze the  $p_T$  spectra of hadrons using a Tsallis distribution [14, 15] characterized by two parameters  $T$  and  $q$  [16]. While the  $T$  parameter corresponds to the kinetic freeze-out temperature in heavy ion collisions, where particles stop interacting elastically, its interpretation in  $p + p$  collisions is less clear compared to different types of collisions. The parameter  $q$ , known as the nonextensive parameter indicates how much the system deviates from complete thermalization [17]. It captures variations in the system's temperature [18–20]. The Tsallis distribution, which models systems close to thermal equilibrium, resembles Hagedorn's power law, which is employed in hard scattering processes in QCD [21, 22].

This work focuses on the  $p_T$  distribution of charged hadrons in  $p + p$ ,  $p + Pb$  and  $Pb + Pb$  collisions at  $\sqrt{s_{NN}} = 5.02$  TeV from the data of ATLAS collaboration [23] in the rapidity range of  $-2.5 < y < 2.0$ . We employ the new Modified Tsallis distribution to describe the transverse flow and in medium energy loss [24, 25] of hadrons in the medium. Both systematic and statistical uncertainties are combined and incorporated into the fitting process.

## 2 Tsallis/Hagedorn distribution function and the modification

The transverse mass ( $m_T = \sqrt{p_T^2 + m^2}$ ) distribution of particles produced in hadronic collisions can be described by the Hagedorn function which is a QCD-inspired summed power law [21] given as

$$E \frac{d^3 N}{dp^3} = A \left( 1 + \frac{m_T}{p_0} \right)^{-n}. \quad (1)$$

This function describes both the bulk spectra in the low  $m_T$  region and the particles produced in QCD hard scatterings reflected in the high  $p_T$  region. Let us compare this function with the Tsallis distribution [14, 15] of thermodynamic origin given by

$$E \frac{d^3 N}{dp^3} = C_n m_T \left( 1 + (q-1) \frac{m_T}{T} \right)^{-1/(q-1)}. \quad (2)$$

The Tsallis distribution describes near-thermal systems in terms of Tsallis parameter  $T$  and the parameter  $q$  which measures degree of non-thermalization [17]. The functions in Eq. 1 and in Eq. (2) have similar mathematical forms with  $n = 1/(q-1)$  and  $p_0 = nT$ . Larger values of  $n$  correspond to smaller values of  $q$ . Both  $n$  and  $q$  have been interchangeably used in Tsallis distribution [15, 26–29]. Phenomenological studies suggest that, for quark-quark point scattering,  $n \sim 4$  [30, 31], which grows larger if multiple scattering centers are involved. The study in Ref. [32] suggests that both the forms given in Eq. 1 and in Eq. (2) give equally good fit to the hadron spectra in  $p + p$  collisions. We use Eq. (2) in case of  $p + p$  collisions.

Tsallis/Hagedorn function is able to describe  $p_T$  spectra in  $p + p$  collisions practically at all generations of proton colliders. There have been many attempts to use the Tsallis distribution in heavy ion collisions as well by including the transverse collective flow [33–35]. In addition, in heavy ion collisions, particle spectra at high  $p_T$  are known to be modified due to in-medium energy loss. The Tsallis/Hagedorn distribution can be modified by including these final state effects in different  $p_T$  regions as follows:

$$E \frac{d^3 N}{dp^3} = A_1 \left[ \exp \left( -\frac{\beta p_T}{p_1} \right) + \frac{m_T}{p_1} \right]^{-n_1} \quad : \quad p_T < p_{T_{\text{th}}} \quad (3a)$$

$$E \frac{d^3 N}{dp^3} = A_2 \left[ \frac{B}{p_2} \left( \frac{p_T}{q_0} \right)^\alpha + \frac{m_T}{p_2} \right]^{-n_2} \quad : \quad p_T > p_{T_{\text{th}}} \quad (3b)$$

The first function (Eq. 3a) is shown to govern the thermal and collective part of the hadron spectrum with the temperature  $T = p_1/n_1$  and the average transverse flow velocity  $\beta$  [34].

The second function (Eq. 3b) is obtained after shifting the distribution in Eq.1 by energy loss  $\Delta m_T$  in the medium as

$$E \frac{d^3 N}{dp^3} = A_2 \left[ 1 + \frac{m_T + \Delta m_T}{p_2} \right]^{-n_2}. \quad (4)$$

The energy loss  $\Delta m_T$  is proportional to  $p_T$  at low  $p_T$  and in general can be parameterized similar to the work in Ref. [36] as

$$\Delta m_T = B \left( \frac{p_T}{q_0} \right)^\alpha. \quad (5)$$

Here, the parameter  $\alpha$  quantifies different energy loss regimes for light quarks in the medium [37, 38]. The parameter  $B$  is proportional to the medium size and  $q_0$  is an arbitrary scale set as 1 GeV. Using Eq. (5) in Eq. 4 and ignoring 1 we get Eq. (3b) applicable for high  $p_T$ . In our study, we find that this function describes the particle spectra at  $p_{T_{th}}$  above 7 GeV/c. Fits to the data would constrain the value of  $B/p_2$  and thus  $p_2$  is not an independent parameter. The empirical parton energy loss in nuclear collisions at RHIC energies is found to be proportional to  $p_T$  [39].

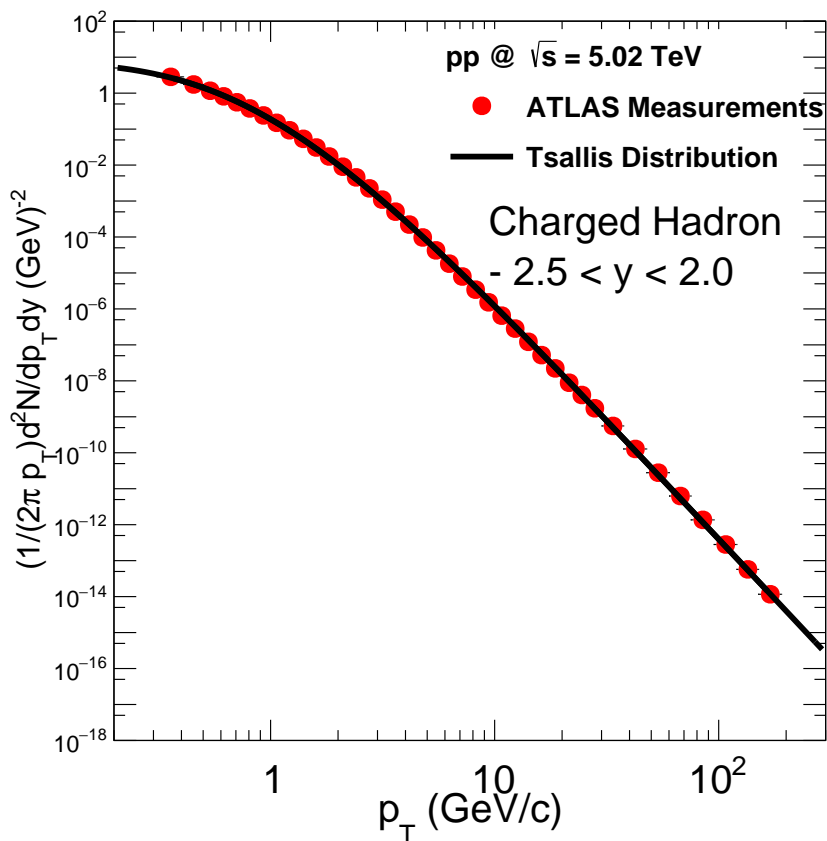
### 3 Results and discussions

#### 3.1 $p + Pb$ collisions at $\sqrt{s_{NN}} = 5.02$ TeV

Figure (1) shows the invariant yields of the charged particles as a function of  $p_T$  for  $p + p$  collisions at  $\sqrt{s} = 5.02$  TeV measured by the ATLAS experiment [23]. The solid curves are the Tsallis distributions fitted to the spectra. The Tsallis distribution function gives good description of the data for both the collision energies which can be inferred from the values of  $\chi^2/NDF$  given in the Table (1).

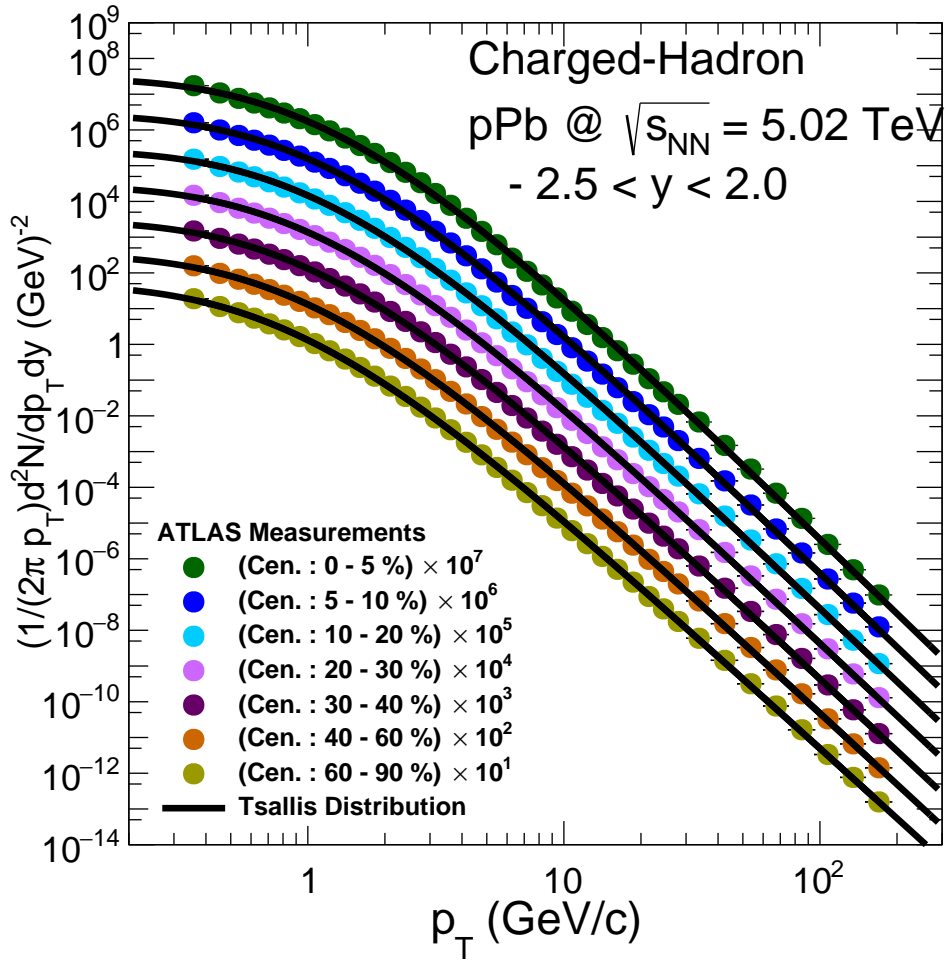
Figure (2) shows the invariant yields of the charged particles as a function of  $p_T$  for different centrality classes in  $p + Pb$  collisions at  $\sqrt{s_{NN}} = 5.02$  TeV measured by the ATLAS experiment [23]. The solid curves are the fitted Tsallis distributions. Figure (3) shows the ratio of the data and the fitted Tsallis distribution as a function of  $p_T$  for  $p + Pb$  collisions at  $\sqrt{s_{NN}} = 5.02$  TeV. ATLAS measured data of  $p + Pb$  and  $p + p$  collisions show deviations from the fit which can be inferred from the values of  $\chi^2/NDF$  given in the Table (2).

Figure (4) shows the invariant yields of the charged particles as a function of  $p_T$  for different centrality classes in  $p + Pb$  collisions at  $\sqrt{s_{NN}} = 5.02$  TeV measured by the ATLAS experiment [23]. The solid curves are the modified Tsallis distributions given by Eq. (3a and 3b). Figure (5) shows the ratio of the data and the fit function by the modified Tsallis distribution as a function of  $p_T$  for different centrality classes in  $p + Pb$  collisions at  $\sqrt{s_{NN}} =$

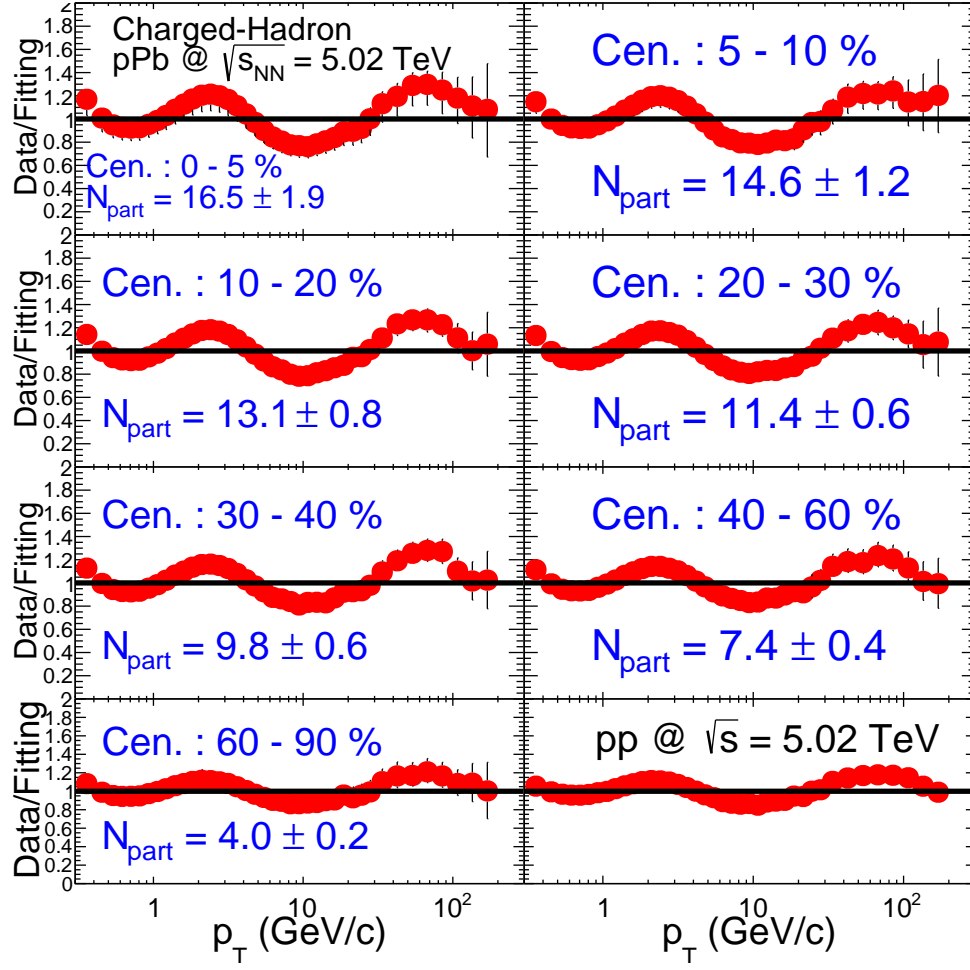


**Fig. 1** The invariant yields of the charged particles as a function of transverse momentum  $p_T$  for  $p + p$  collision at  $\sqrt{s} = 5.02$  TeV measured by the ATLAS experiment [23]. The solid curves are the fitted Tsallis distribution functions.

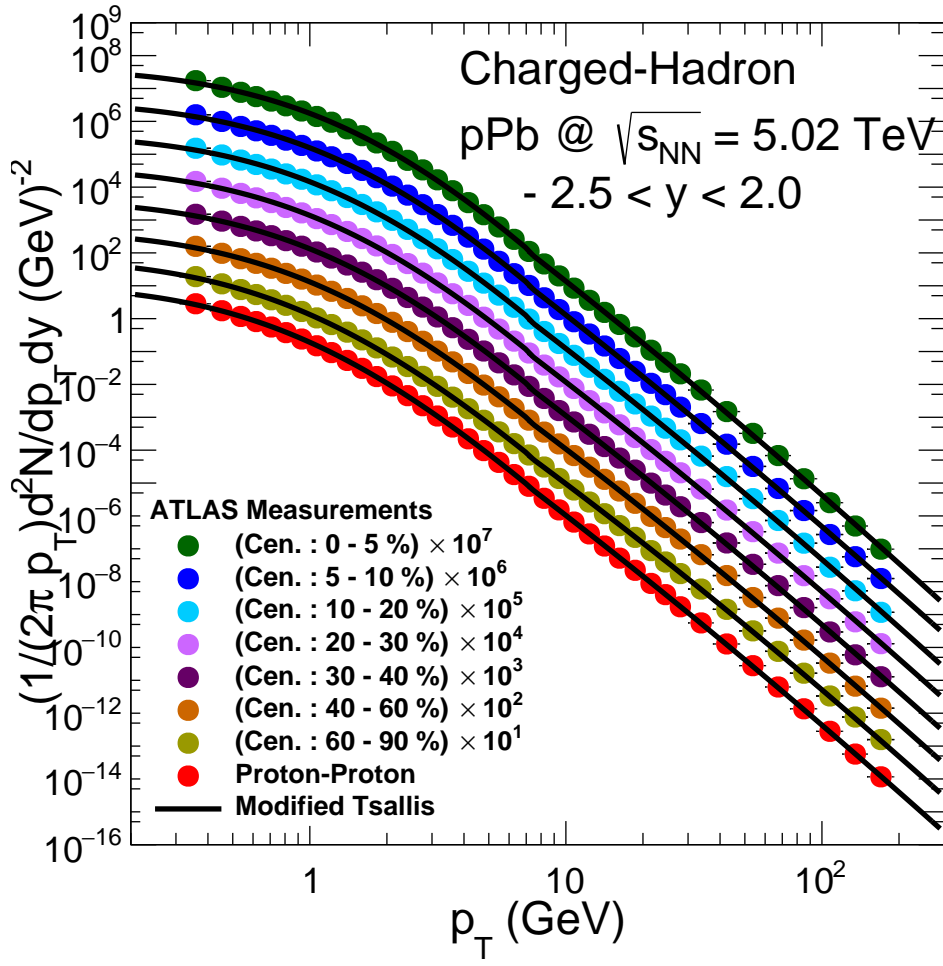
5.02 TeV. The ratio of the data and the fit function shows that modified Tsallis distribution function gives excellent description of the measured data in full  $p_T$  range for all centrality classes. The parameters of the modified Tsallis distribution are given in the Table (3). The values of the first set of parameters ( $n_1$ ,  $p_1$ ,  $\beta$ ) are constant for different range of pseudorapidities. While fitting the second function, we fix the parameter  $n_2 = 7.67$  guided by  $p + p$  value. The exponent  $\alpha$  which decides the variation of the energy loss of partons as a function of their energy remains same. In conclusion, the function given in Eq. (3a and 3b) gives excellent description of the hadron spectra over wide range of  $p_T$  with its parameters indicating different physics effects in the  $p + Pb$  collisions.



**Fig. 2** The invariant yields of the charged particles as a function of the transverse momentum  $p_T$  for different centrality classes in  $p + Pb$  collisions at  $\sqrt{s_{NN}} = 5.02$  TeV measured by the ATLAS experiment [23]. The solid curves are the fitted Tsallis distribution functions.

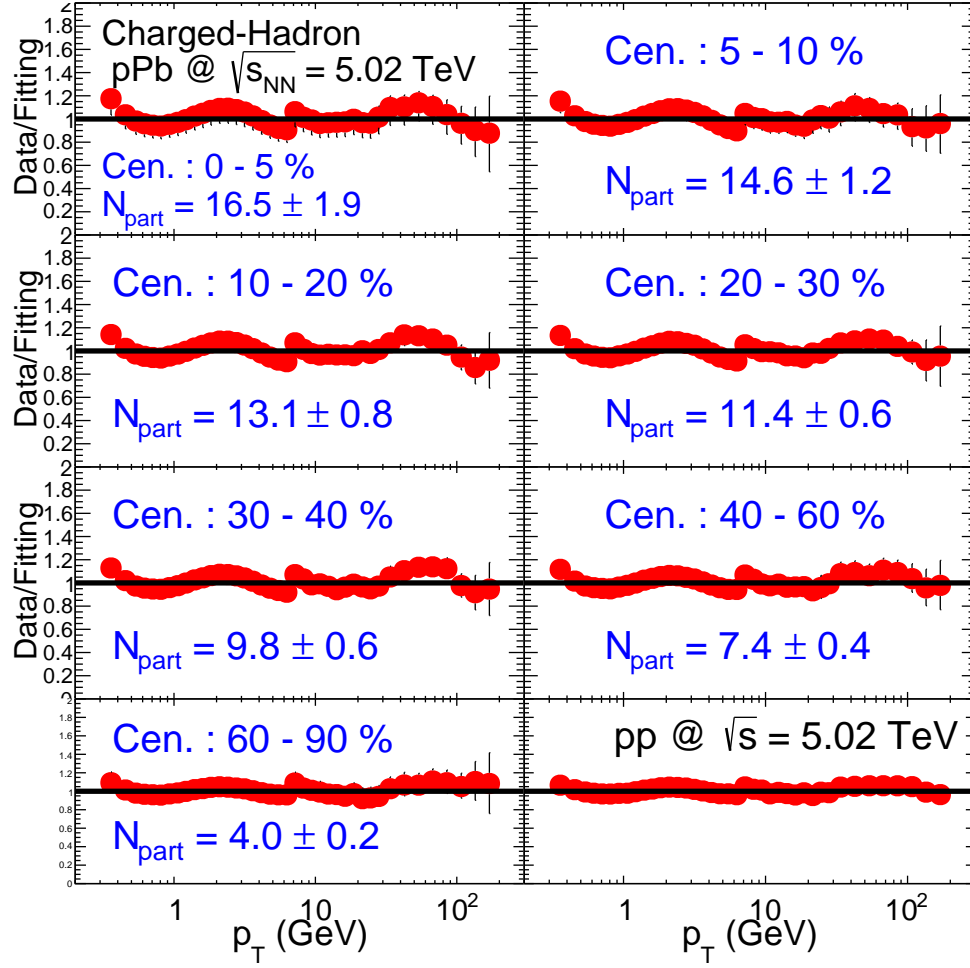


**Fig. 3** The ratio of the charged particles yields data and their Tsallis fits as a function of the transverse momentum  $p_T$  for different centrality classes in  $p + Pb$  collisions at  $\sqrt{s_{NN}} = 5.02$  TeV.



**Fig. 4** The invariant yields of the charged particles as a function of the transverse momentum  $p_T$  for different centrality classes in  $p + Pb$  collisions at  $\sqrt{s_{\text{NN}}} = 5.02 \text{ TeV}$  measured by the ATLAS experiment [23]. The solid curves are the modified Tsallis distributions (Eq. 3a).

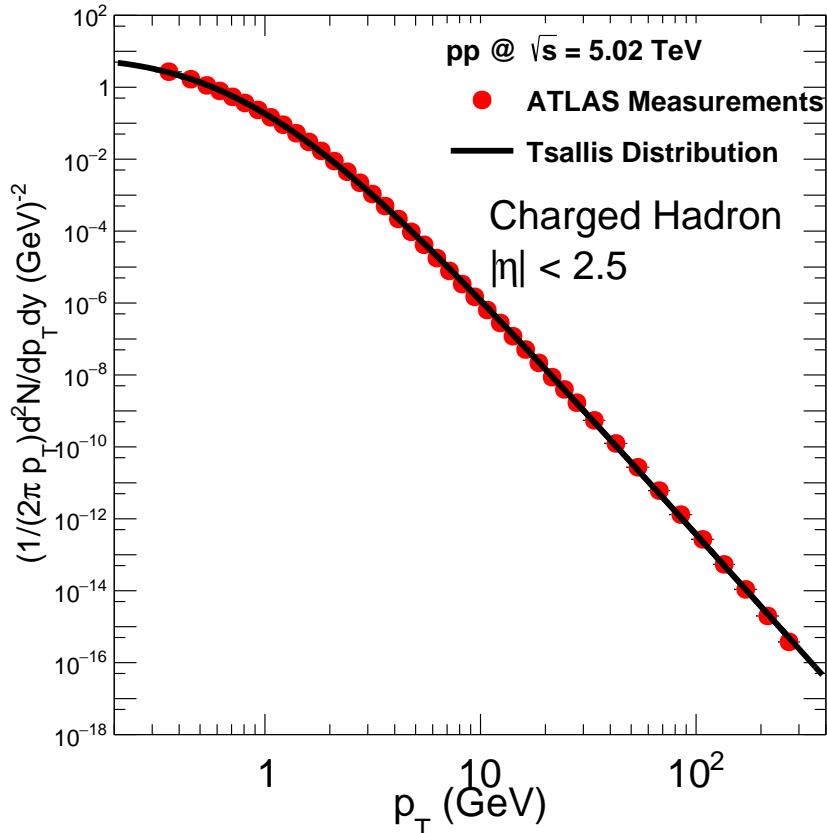




**Fig. 5** The ratio of the charged particle yield data and the fit function (Modified Tsallis distribution Eq. 3a) as a function of the transverse momentum  $p_T$  for different centrality classes in  $p + Pb$  collisions at  $\sqrt{s_{NN}} = 5.02$  TeV.

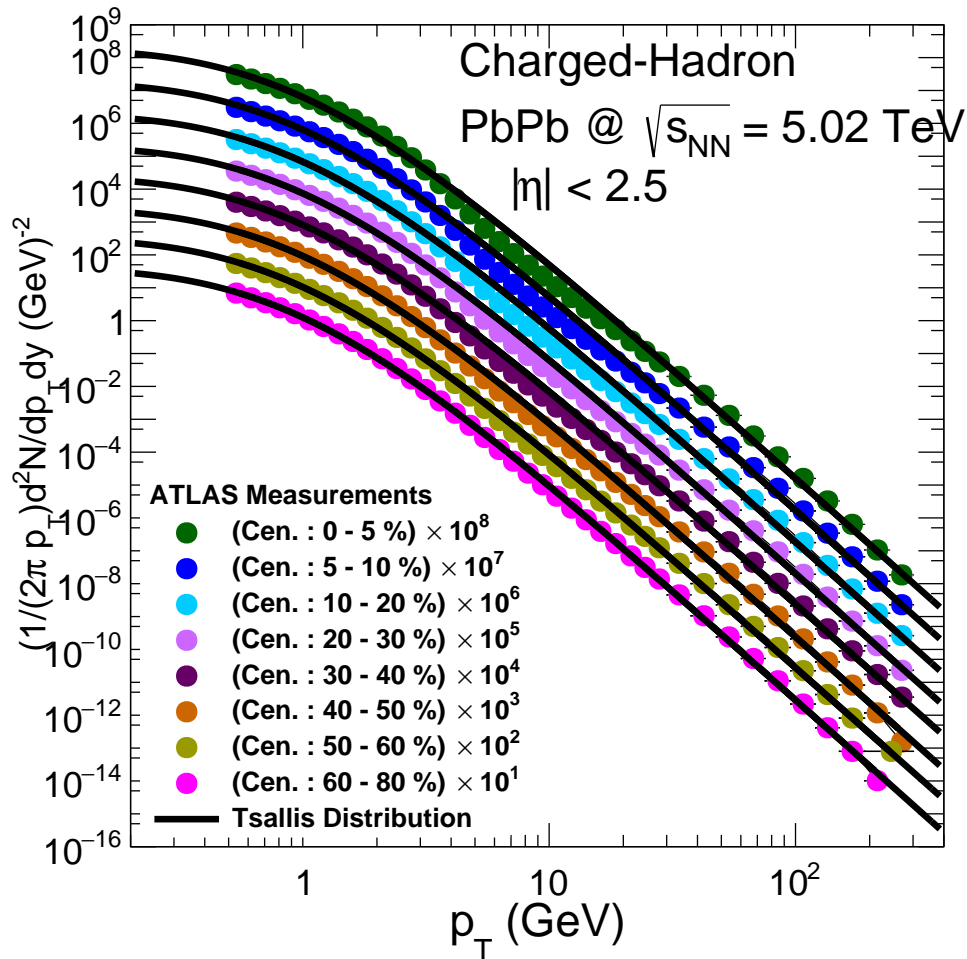
### 3.2 $Pb + Pb$ collisions at $\sqrt{s_{NN}} = 5.02$ TeV

Figure (6) shows the invariant yields of the charged particles as a function of  $p_T$  for  $p + p$  collisions at  $\sqrt{s} = 5.02$  TeV measured by the ATLAS experiment [23]. The solid curves are the Tsallis distributions fitted to the spectra. The Tsallis distribution function gives good description of the data for both the collision energies which can be inferred from the values of  $\chi^2/\text{NDF}$  given in the Table (4).



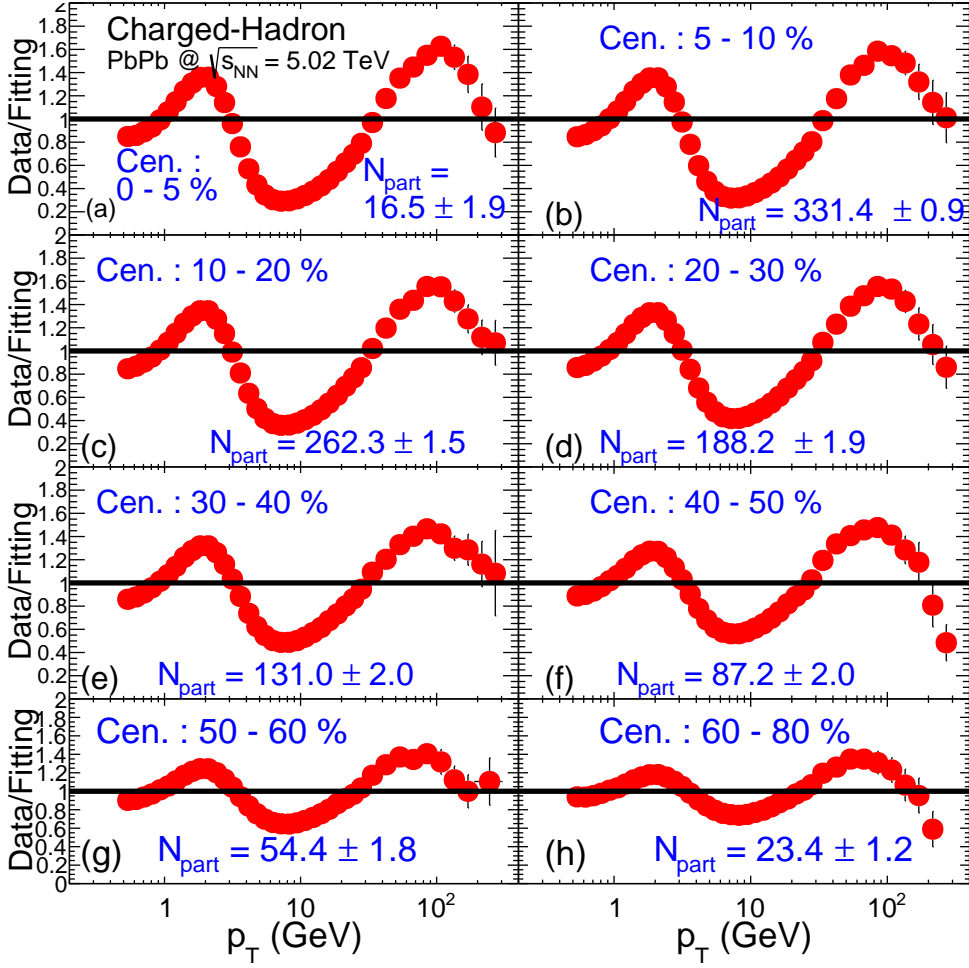
**Fig. 6** The invariant yields of the charged particles as a function of transverse momentum  $p_T$  for  $p + p$  collision at  $\sqrt{s} = 5.02$  TeV measured by the ATLAS experiment [23]. The solid curves are the fitted Tsallis distribution functions.

Figure (7) shows the invariant yields of the charged particles as a function of  $p_T$  for different centrality classes in  $Pb + Pb$  collisions at  $\sqrt{s_{NN}} = 5.02$  TeV measured by the ATLAS experiment [23]. The solid curves are the fitted Tsallis distributions. Figure (8) shows the ratio of the data and the fitted Tsallis distribution as a function of  $p_T$  for  $Pb + Pb$  collisions at  $\sqrt{s_{NN}} = 5.02$  TeV. ATLAS measured data of  $Pb + Pb$  and  $p + p$  collisions show deviations from the fit which can be inferred from the values of  $\chi^2/\text{NDF}$  given in the Table (5).



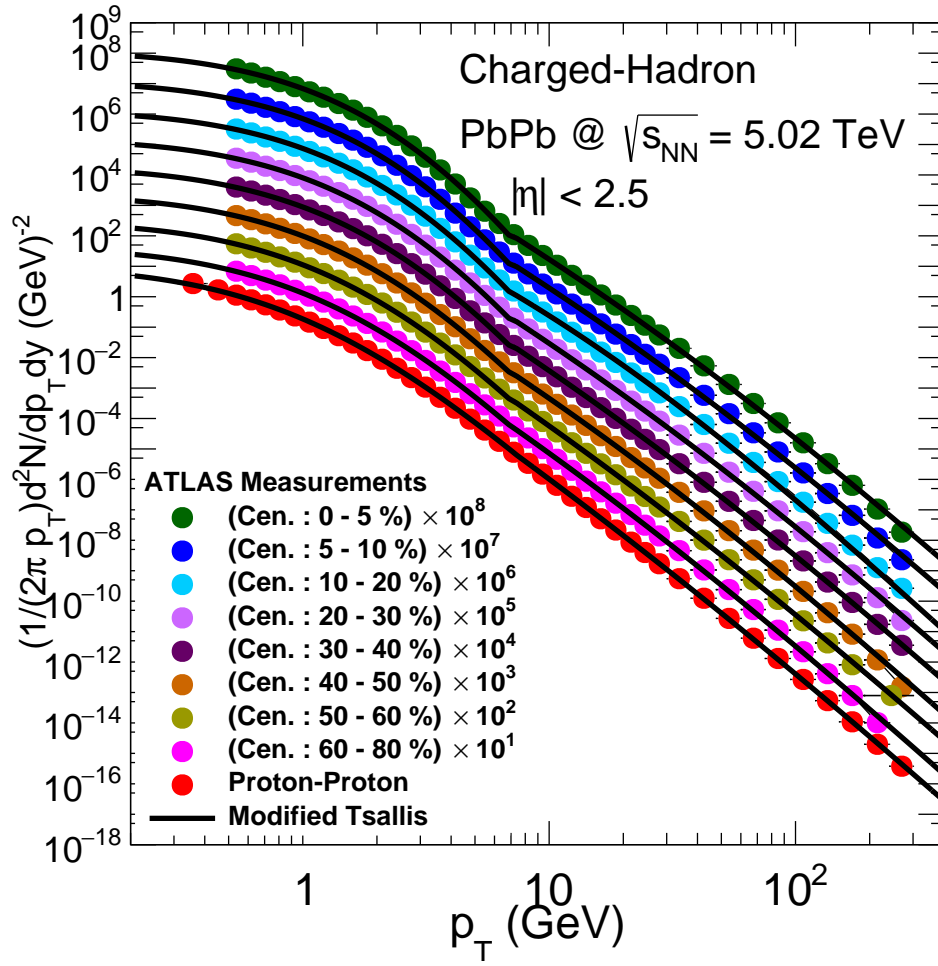
**Fig. 7** The invariant yields of the charged particles as a function of the transverse momentum  $p_T$  for different centrality classes in  $Pb + Pb$  collisions at  $\sqrt{s_{\text{NN}}} = 5.02 \text{ TeV}$  measured by the ATLAS experiment [23]. The solid curves are the fitted Tsallis distribution functions.

Figure (9) shows the invariant yields of the charged particles as a function of  $p_T$  for different centrality classes in  $Pb + Pb$  collisions at  $\sqrt{s_{\text{NN}}} = 5.02 \text{ TeV}$  measured by the ATLAS experiment [23]. The solid curves are the modified Tsallis distributions given by Eq. (3a and 3b). Figure (10) shows the ratio of the data and the fit function by the modified Tsallis distribution as a function of  $p_T$  for different centrality classes in  $Pb + Pb$  collisions at  $\sqrt{s_{\text{NN}}} = 5.02 \text{ TeV}$ . The ratio of the data and the fit function shows that modified Tsallis distribution function gives excellent description of the measured data in full  $p_T$  range for all centrality classes. The parameters of the modified Tsallis distribution are given in the Table (6). The values of the first set of parameters ( $n_1, p_1, \beta$ ) are constant for different range of pseudorapidities. While fitting the second function, we fix the parameter  $n_2 = 7.70$  guided by  $p +$



**Fig. 8** The ratio of the charged particles yields data and their Tsallis fits as a function of the transverse momentum  $p_T$  for different centrality classes in  $Pb + Pb$  collisions at  $\sqrt{s_{NN}} = 5.02$  TeV.

$p$  value. The exponent  $\alpha$  which decides the variation of the energy loss of partons as a function of their energy remains same. In conclusion, the function given in Eq. ( 3a and 3b) gives excellent description of the hadron spectra over wide range of  $p_T$  with its parameters indicating different physics effects in the  $Pb + Pb$  collisions.



**Fig. 9** The invariant yields of the charged particles as a function of the transverse momentum  $p_T$  for different centrality classes in  $Pb + Pb$  collisions at  $\sqrt{s_{\text{NN}}} = 5.02 \text{ TeV}$  measured by the ATLAS experiment [23]. The solid curves are the modified Tsallis distributions (Eq. 3a).

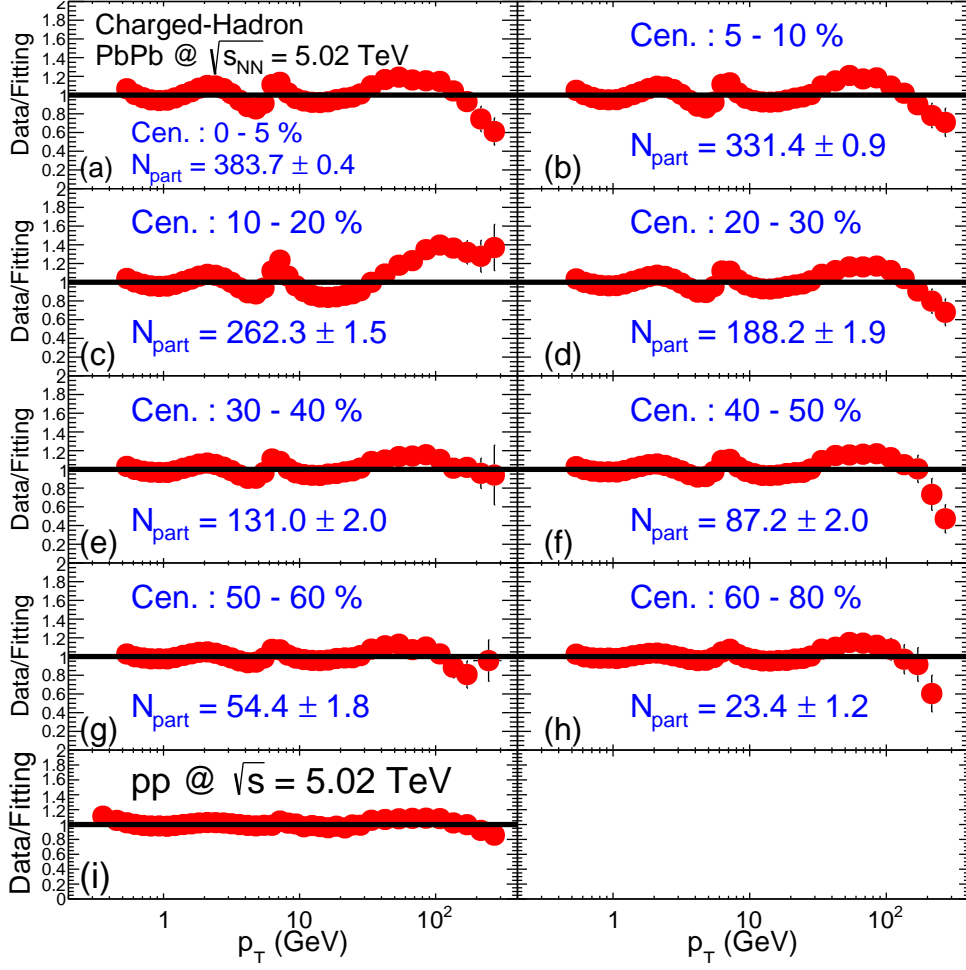


**Fig. 10** The ratio of the charged particle yield data and the fit function (Modified Tsallis distribution Eq. 3a) as a function of the transverse momentum  $p_T$  for different centrality classes in  $Pb + Pb$  collisions at  $\sqrt{s_{NN}} = 5.02$  TeV.

## 4 Conclusion

In the article, we carried out an analysis of transverse momentum spectra of charged hadron in  $p + Pb$ , and  $Pb + Pb$  collisions at  $\sqrt{s_{\text{NN}}} = 5.02$  TeV. We first use the Tsallis distribution to describe the  $p_{\text{T}}$  spectra of charged hadrons in  $p + Pb$  and  $Pb + Pb$  collisions. We found that Tsallis distribution does not describe the  $p_{\text{T}}$  spectra properly. We see a suppression of  $p_{\text{T}}$  spectra above  $7\text{GeV}/c$ . To describe and explain the  $p_{\text{T}}$  spectra of the charged hadrons, we use the modified Tsallis distribution by incorporating the medium effects. Here we fit the  $p_{\text{T}}$  spectra of charged hadrons in different centralities of  $p + Pb$  and  $Pb + Pb$  collisions at  $\sqrt{s_{\text{NN}}} = 5.02$  TeV using modified Tsallis distribution. We observe the effect of transverse flow in the low-to-intermediate  $p_{\text{T}}$  region ( $p_{\text{T}} \leq 7.0$  GeV/ $c$ ) and in-medium energy loss in the high  $p_{\text{T}}$  region ( $p_{\text{T}} > 7\text{GeV}/c$ ). We found that in the low (to intermediate)  $p_{\text{T}}$  region the parameters  $n_1, p_1$  and  $\beta$  are more in central collisions and are gradually decreasing towards peripheral collisions. This is due to the larger number of multi-scatterings phenomena occurring among partons in the central collisions than the peripheral collisions. So there is a transverse collective flow observed among particles in this region. In the high  $p_{\text{T}}$  region the exponent  $\alpha$  which decides the variation of the energy loss of partons as a function of their energy remains within 0.59 to 0.73 in  $p + Pb$  collisions at  $\sqrt{s_{\text{NN}}} = 5.02$  TeV, 0.32 to 0.59 in  $Pb + Pb$  collisions at  $\sqrt{s_{\text{NN}}} = 5.02$  TeV. So, finally, we can say that a simple modification in the Tsallis distribution gives excellent description of charged particle spectra with its parameters having potential to quantify various in-medium effects in  $p + Pb$  and  $Pb + Pb$  collisions.

5 Appendix :: Table :  $p + Pb$  collisions  $\sqrt{s_{\text{NN}}} = 5.02$  TeV

**Table 1** The parameters of the Tsallis function obtained by fitting the charged particles transverse momentum ( $p_{\text{T}}$ ) spectrum in  $p + p$  collision at  $\sqrt{s} = 5.02$  TeV.

Rapidity ( $y$ )	$n$	$q$	$T$ (MeV)	$\frac{\chi^2}{\text{NDF}}$
$- 2.5 < y < 2.0$	$7.67 \pm 0.10$	1.13	$84.78 \pm 5.46$	0.05

**Table 2** The parameters of the Tsallis function obtained by fitting the charged particles transverse momentum ( $p_{\text{T}}$ ) spectrum in  $p + Pb$  collisions  $\sqrt{s_{\text{NN}}} = 5.02$  TeV.

Centrality (%)	$N_{\text{part}}$	$n$	$q$	$T$ (MeV)	$\frac{\chi^2}{\text{NDF}}$
0 - 5	$16.50 \pm 1.90$	$7.97 \pm 0.11$	1.13	$116.26 \pm 5.98$	0.16
5 - 10	$14.60 \pm 1.20$	$7.88 \pm 0.11$	1.13	$112.85 \pm 6.14$	0.15
10 - 20	$13.10 \pm 0.80$	$7.83 \pm 0.10$	1.13	$110.56 \pm 5.40$	0.14
20 - 30	$11.40 \pm 0.60$	$7.77 \pm 0.10$	1.13	$107.15 \pm 5.54$	0.13
30 - 40	$9.80 \pm 0.60$	$7.73 \pm 0.10$	1.13	$104.12 \pm 5.56$	0.11
40 - 60	$7.40 \pm 0.40$	$7.65 \pm 0.10$	1.13	$98.44 \pm 5.70$	0.09
60 - 90	$4.00 \pm 0.20$	$7.53 \pm 0.10$	1.13	$86.65 \pm 5.77$	0.05



**Table 3** The parameters of the modified Tsallis function Eq.( 3a and 3b) obtained by fitting the charged particle spectra in  $p + Pb$  collisions at  $\sqrt{s_{\text{NN}}} = 5.02$  TeV.

System	Centrality (%)	$N_{\text{part}}$	$n_1$	$p_1$ (GeV/c)	$\beta$	$\alpha$	$B$ (GeV/c)	$\frac{\chi^2}{\text{NDF}}$
$p + Pb$	0 - 5	$16.50 \pm 1.90$	$7.69 \pm 2.21$	$1.38 \pm 1.55$	$0.13 \pm 0.55$	$0.59 \pm 0.27$	$2.40 \pm 0.75$	0.05
$p + Pb$	5 - 10	$14.60 \pm 1.20$	$7.36 \pm 0.84$	$1.23 \pm 0.28$	$0.15 \pm 0.30$	$0.63 \pm 0.25$	$2.76 \pm 1.35$	0.05
$p + Pb$	10 - 20	$13.10 \pm 0.80$	$7.32 \pm 1.88$	$1.22 \pm 0.79$	$0.13 \pm 0.12$	$0.59 \pm 0.13$	$2.72 \pm 0.47$	0.05
$p + Pb$	20 - 30	$11.40 \pm 0.60$	$7.20 \pm 2.19$	$1.16 \pm 0.81$	$0.13 \pm 0.19$	$0.60 \pm 0.05$	$2.90 \pm 0.38$	0.04
$p + Pb$	30 - 40	$9.80 \pm 0.60$	$7.12 \pm 1.96$	$1.11 \pm 0.68$	$0.13 \pm 0.10$	$0.60 \pm 0.05$	$2.95 \pm 0.38$	0.04
$p + Pb$	40 - 60	$7.40 \pm 0.40$	$6.99 \pm 2.03$	$1.02 \pm 0.64$	$0.13 \pm 0.09$	$0.59 \pm 0.05$	$3.08 \pm 0.39$	0.03
$p + Pb$	60 - 90	$4.00 \pm 0.20$	$6.78 \pm 2.30$	$0.86 \pm 0.45$	$0.12 \pm 0.10$	$0.57 \pm 0.04$	$3.26 \pm 0.39$	0.02
$p + p$	-	-	$6.94 \pm 2.36$	$0.86 \pm 1.17$	$0.12 \pm 0.10$	$0.61 \pm 0.05$	$2.92 \pm 0.37$	0.01

6 Appendix :: Table :  $Pb + Pb$  collisions  $\sqrt{s_{NN}} = 5.02$  TeV

**Table 4** The parameters of the Tsallis function obtained by fitting the charged particles transverse momentum ( $p_T$ ) spectrum in  $p + p$  collision at  $\sqrt{s} = 5.02$  TeV.

Rapidity ( $y$ )	$n$	$q$	$T$ (MeV)	$\frac{\chi^2}{\text{NDF}}$
$- 2.5 < y < 2.0$	$7.70 \pm 0.09$	1.13	$86.19 \pm 5.31$	0.05

**Table 5** The parameters of the Tsallis function obtained by fitting the charged particles transverse momentum ( $p_T$ ) spectrum in  $Pb + Pb$  collisions  $\sqrt{s_{NN}} = 5.02$  TeV.

Centrality (%)	$N_{\text{part}}$	$n$	$q$	$T$ (MeV)	$\frac{\chi^2}{\text{NDF}}$
0 - 5	$383.70 \pm 0.40$	$7.71 \pm 0.07$	1.13	$94.07 \pm 5.22$	1.05
5 - 10	$331.40 \pm 0.90$	$7.70 \pm 0.10$	1.13	$95.28 \pm 8.90$	0.98
10 - 20	$262.30 \pm 1.50$	$7.70 \pm 0.12$	1.13	$95.85 \pm 11.09$	0.87
20 - 30	$188.20 \pm 1.90$	$7.71 \pm 0.10$	1.13	$96.33 \pm 8.36$	0.73
30 - 40	$131.00 \pm 2.00$	$7.67 \pm 0.09$	1.13	$94.27 \pm 7.99$	0.58
40 - 50	$87.20 \pm 2.00$	$7.71 \pm 0.10$	1.13	$95.12 \pm 7.83$	0.43
50 - 60	$54.40 \pm 1.80$	$7.68 \pm 0.11$	1.13	$92.76 \pm 7.63$	0.29
60 - 80	$23.40 \pm 1.20$	$7.72 \pm 0.11$	1.13	$92.51 \pm 7.39$	0.16

**Table 6** The parameters of the modified Tsallis function Eq.( 3a and 3b) obtained by fitting the charged particle spectra in  $Pb + Pb$  collisions at  $\sqrt{s_{NN}} = 5.02$  TeV.

System	Centrality (%)	$N_{\text{part}}$	$n_1$	$p_1$ (GeV/c)	$\beta$	$\alpha$	$B$ (GeV/c)	$\frac{\chi^2}{\text{NDF}}$
$Pb + Pb$	0 - 5	$383.70 \pm 0.40$	$10.85 \pm 0.43$	$2.00 \pm 1.77$	$0.28 \pm 0.10$	$0.49 \pm 0.05$	$4.97 \pm 0.57$	0.06
$Pb + Pb$	5 - 10	$331.40 \pm 0.90$	$10.72 \pm 0.44$	$2.00 \pm 1.06$	$0.27 \pm 0.10$	$0.50 \pm 0.13$	$4.83 \pm 0.71$	1.29
$Pb + Pb$	10 - 20	$262.30 \pm 1.50$	$10.56 \pm 0.47$	$2.00 \pm 1.03$	$0.25 \pm 0.11$	$0.32 \pm 0.06$	$4.61 \pm 0.67$	1.28
$Pb + Pb$	20 - 30	$188.20 \pm 1.90$	$10.35 \pm 0.72$	$2.00 \pm 1.23$	$0.21 \pm 0.12$	$0.50 \pm 0.14$	$4.26 \pm 0.60$	0.07
$Pb + Pb$	30 - 40	$131.00 \pm 2.00$	$10.09 \pm 0.96$	$2.00 \pm 1.41$	$0.15 \pm 0.09$	$0.52 \pm 0.12$	$4.02 \pm 0.55$	0.02
$Pb + Pb$	40 - 50	$87.20 \pm 2.00$	$8.61 \pm 4.54$	$1.43 \pm 1.27$	$0.24 \pm 0.13$	$0.48 \pm 0.17$	$3.61 \pm 0.49$	1.16
$Pb + Pb$	50 - 60	$54.40 \pm 1.80$	$7.96 \pm 4.10$	$1.22 \pm 0.83$	$0.24 \pm 0.17$	$0.55 \pm 0.16$	$3.56 \pm 0.77$	0.02
$Pb + Pb$	60 - 80	$23.40 \pm 1.20$	$7.60 \pm 2.35$	$1.11 \pm 0.85$	$0.19 \pm 0.13$	$0.52 \pm 0.21$	$3.01 \pm 0.52$	0.02
$p + p$	-	-	$7.45 \pm 0.52$	$1.11 \pm 0.74$	$0.02 \pm 0.01$	$0.59 \pm 0.12$	$2.86 \pm 0.65$	0.01

## References

- [1] PHENIX Collab. (K. Adcox *et al.*), *Nucl. Phys. A* **757**, 184-283 (2005).
- [2] STAR Collab. (J. Adams *et al.*), *Nucl. Phys. A* **757**, 102-183 (2005).
- [3] LHC Collab. (N. Armesto *et al.*), *J. Phys. G* **35**, 054001 (2008).
- [4] E. V. Shuryak, *Phys. Rept.* **61**, 71–158 (1980).
- [5] K. A. Olive, *Science* **251**, 1194–1199 (1991).
- [6] D. J. Schwarz, *Annalen Phys* **12**, 220–270 (2003).
- [7] F. Becattini and U. Heinz, *Z. Phys. C* **76**, 269 (1997).
- [8] V. Khachatryan *et al.*, (CMS Collaboration), *JHEP* **09**, 091 (2010) arXiv:1009.4122 [hep-ex].
- [9] J. Adam *et al.* (ALICE Collaboration), *Nature Phys.* **13**, 535 (2017).
- [10] T. Hirano and Y. Nara, *Phys. Rev. C* **69**, 034908 (2004).
- [11] R. Fries *et al.* *Ann. Rev. Nucl. Part. Sci.* **58** 177-205 (2008), *Phys. Rev. Lett.* **90**, 202303 (2003), *Phys. Rev. C* **68**, 044902 (2003), *J. Phys. G* **30** S223-S228 (2004).
- [12] R. Fries *J. Phys. G* **30** S853-S860 (2004).
- [13] X. N. Wang *Phys. Lett. B* **579**, 299 (2004).
- [14] C. Tsallis, *J. Statist. Phys.* **52** 479 (1988).
- [15] T. S. Biro, G. Purcsel and K. Urmosy, *Eur. Phys. J. A* **40** 325 (2009). [arXiv:0812.2104 [hep-ph]].
- [16] A. Adare *et al.*, PHENIX Collaboration, *Phys. Rev. D* **83** 052004 (2011).
- [17] G. Wilk and Z. Wlodarczyk, *Phys. Rev. Lett.* **84**, 2770 (2000).
- [18] P. K. Khandai, P. Sett, P. Shukla and V. Singh, *Int. J. Mod. Phys. A* **28** (2013) 1350066.
- [19] C. Y. Wong and G. Wilk, *Acta Phys. Polon. B* **43** 2047 (2012), [arXiv:1210.3661 [hep-ph]].
- [20] C. Y. Wong and G. Wilk, *Phys. Rev. D* **87** 114007 (2013), [arXiv:1305.2627 [hep-ph]].
- [21] R. Hagedorn, *Riv. Nuovo Cim.* **6N10** 1 (1983).
- [22] R. Blankenbecler and S. J. Brodsky, *Phys. Rev. D* **10** 2973 (1974).
- [23] [ATLAS], [arXiv:2211.15257 [hep-ex]].
- [24] K. Saraswat, P. Shukla and V. Singh, *J. Phys. Commun.* **2** 035003 (2018).
- [25] P. Kumar, P. K. Khandai, Kapil Saraswat and V. Singh, *Int. J. Mod. Phys. A* **36** 2150059 (2021),
- [26] J. Cleymans and D. Worku, *Eur. Phys. J. A* **48** (2012) 160, [arXiv:1203.4343 [hep-ph]].
- [27] A. Adare *et al.* [PHENIX Collaboration], *Phys. Rev. C* **83** (2011) 064903, [arXiv:1102.0753 [nucl-ex]].
- [28] B. I. Abelev *et al.* [STAR Collaboration], *Phys. Rev. C* **75** (2007) 064901, [nucl-ex/0607033].
- [29] A. Adare *et al.* [PHENIX Collaboration], *Phys. Rev. D* **83** (2011) 052004, [arXiv:1005.3674 [hep-ex]].
- [30] R. Blankenbecler, S. J. Brodsky and J. F. Gunion, *Phys. Rev. D* **12** (1975) 3469.
- [31] S. J. Brodsky, H. J. Pirner and J. Raufeisen, *Phys. Lett. B* **637** (2006) 58, [hep-ph/0510315].
- [32] H. Zheng and L. Zhu, *Adv. High Energy Phys.* **2016** (2016) 9632126, [arXiv:1512.03555 [nucl-th]].
- [33] Z. Tang, Y. Xu, L. Ruan, G. van Buren, F. Wang and Z. Xu, *Phys. Rev. C* **79** (2009) 051901, [arXiv:0812.1609 [nucl-ex]].
- [34] P. K. Khandai, P. Sett, P. Shukla and V. Singh, *J. Phys. G* **41** (2014) 025105, [arXiv:1310.4022 [nucl-th]].
- [35] P. Sett and P. Shukla, *Int. J. Mod. Phys. E* **24** (2015) 1550046, [arXiv:1505.05258 [hep-ph]].
- [36] M. Spousta, *Phys. Lett. B* **767** (2017) 10, [arXiv:1606.00903 [hep-ph]].
- [37] R. Baier, D. Schiff and B. G. Zakharov, *Ann. Rev. Nucl. Part. Sci.* **50** (2000) 37, [hep-ph/0002198].
- [38] S. De and D. K. Srivastava, *J. Phys. G* **39** (2012) 015001, Erratum: [*J. Phys. G* **40** (2013) 049502], [arXiv:1107.5659 [nucl-th]].
- [39] G. Wang and H. Z. Huang, *Phys. Lett. B* **672** (2009) 30, [arXiv:0810.2822 [nucl-ex]].